Results in Physics 37 (2022) 105496

Contents lists available at ScienceDirect

Results in Physics

journal homepage: www.elsevier.com/locate/rinp

Some estimation methods for mixture of extreme value distributions with simulation and application in medicine

Showkat Ahmad Lone [a], Sadia Anwar [b], Tabassum Naz Sindhu [c,*], Fahd Jarad [d,e,**]

[a] Department of Basic Sciences, College of Science and Theoretical, Studies, Saudi Electronic University, (Jeddah-M), Riyadh 11673, Kingdom of Saudi Arabia
[b] Department of Mathematics,College of Arts and Sciences, Wadi Ad Dawasir (11991), Prince Sattam Bin Abdul Aziz University, Al-Kharj, Kingdom of Saudi Arabia
[c] Department of Statistics, Quaid-i-Azam University 45320, Islamabad 44000, Pakistan
[d] Department of Mathematics, Faculty of Arts and Sciences, Cankaya University, 06530 Ankara, Turkey
[e] Department of Medical Research, China Medical University Hospital, China Medical University, Taichung 40402, Taiwan

ARTICLE INFO

Keywords:
Mixture models
Least square estimation
Mills ratio
Weighted least square estimation
Reliability function
Mean square error

ABSTRACT

In recent years, statisticians have grown increasingly engaged in research of mixture models, particularly in the previous decade, without adequate consideration of challenge of estimating the parameters of mixture models from a frequentist perspective. Except for maximum likelihood estimation, this study addresses this vacuum by discussing the two other classical methods of estimation for mixture model. We commence by briefly describing the three frequentist approaches, namely maximum likelihood, ordinary, and weighted least squares, and then comparing them through extensive numerical simulations. The model's applicability is illustrated by its application to simulated and real-world data, which yields promising results in terms of enhanced estimation.

Introduction

The mixture model is noted in the published studies, and it is easy to notice when a statistical population comprises two or more subgroups. Using this concept, we can merge statistical probability models to create a new model that maintains the attributes of its constituents. The mixture representations have been rectified with extreme care in several applicable places. Recent data in applied sciences (engineering, finance, environmental sciences, and so forth) has raised issues of classical models, whose adaptability prohibits them from revealing some important elements. To explore deeper into these restrictions, new mixture distributions have been created. Finite mixture lifetime models have become increasingly popular in recent years in biological, chemical, social science, physical, and other domains because of their methodological improvement and feasible applicability.

A vast number of authors have looked into mixture models and their characteristics. In [1] authors examined classical characteristics of the mixture of Burr XII and Weibull distributions. In [2], the authors combined two inverse Weibull models and studied the properties and parameter estimates in depth. In [3] researcher proposed 2-Component Mixture of Inverse Weibull models (2-CMIWDM) and used graphs of PDF and HRF to analyse some of its characteristics. In [4] researchers concentrated on the shapes of PDF and HRF functions, and also graphical techniques, to investigate the hybrid of two inverse Weibull models. Mohammadi et al. [5], Ateya [6], Mohamed et al. [7], Sindhu et al. [8], Zhang and Huang [9], Sindhu et al. [10–14] are some of the researchers who work with mixture modelling in many practical applications. Some additional interesting research are [15–20]. In many instances, existing data can be seen as a fusion of two or more models. We can use this approach to combine statistical models to create a new one.

The exponential model has a wide range of real-world implications in estimating the lifespan of a device whose lifetime is independent of its age due to its memory less nature. In numerous areas of physics, the exponential model is widely employed to describe specific occurrences. The exponential model is an excellent fit for modelling longevity since the failure rate of several electronic gadgets is regardless of their age.

In literature, there are various estimating methods for parametric distributions, some of which have been widely investigated from a theoretical perspective. It is noteworthy, however, that in situation of small samples, the maximum likelihood estimator (MLE) frequently fails to execute effectively. As a result, new estimation techniques have recently been created. The attraction of estimating methods varies depending on the user and the application area. The goal of this paper is to give a framework for selecting optimum estimation technique

* Corresponding author.
** Corresponding author at: Department of Mathematics, Faculty of Arts and Sciences, Cankaya University, 06530 Ankara, Turkey.
E-mail addresses: sindhuqau@gmail.com (T.N. Sindhu), fahd@cankaya.edu.tr (F. Jarad).

https://doi.org/10.1016/j.rinp.2022.105496
Received 11 March 2022; Received in revised form 7 April 2022; Accepted 8 April 2022
Available online 19 April 2022
2211-3797/© 2022 The Author(s). Published by Elsevier B.V. This is an open access article under the CC BY-NC-ND license (http://creativecommons.org/licenses/by-nc-nd/4.0/).

Nomenclature

Symbols

$f(t\|\breve{\Delta})$	PDF
$R(t\|\breve{\Delta})$	RF
$H(t\|\breve{\Delta})$	CHRF
$Y\left(t\|\breve{\Delta}\right)$	Mill's Ratio
$\tilde{M}_t(\upsilon)$	MGF
$P_t(\omega)$	PGF
$F(t\|\breve{\Delta})$	CDF, FF
$h(t\|\breve{\Delta})$	HRF
$Q(q;\breve{\Delta})$	QF
$R\left(t\|\breve{\Delta}\right)$	RF
$\ddot{M}_t(\upsilon)$	CF
$F_t(\omega)$	FMGF

Abbreviations

QF	Quantile Function
CDF	Cumulative Distribution Function
PGF	Probability Generating Function
MLE	Maximum likelihood Estimator
FMGF	Factorial Moment Generating Function
RF	Reliability Function
MSE	Mean Square Error
WLSE	Weighted Least Square Estimator
CHRF	Cumulative Hazard Rate Function
FF	Failure Function
CF	Characteristic Function
PDF	Probability Density Function
MTTF	Mean Time to Failure
HRF	Hazard Rate Function
MGF	Moment Generating Function
TTF	Time-To-Failure
LSE	Least Square Estimator
MRL	Mean Residual Life
r.v.	Random Variable

for 2-Component Mixture of Exponential Model (2-CMEM), which will be useful to applied statisticians. In the literature, comparisons of estimate techniques for other classical models have been examined, for example, [21–25].

This study is driven by the ubiquitous use of mixture modelling, and we intend to analyse the mixture of Exponential distributions using three classical estimating methods. The main aim of this study is to reveal how different frequentist estimators of the proposed model execute for different sample sizes, as well as to demonstrate that the distribution outperforms than one component distributions for two real data sets. Besides from MLE, we apply two different strategies to estimate the parameters of 2-CMEM in this study, including LSE and WLSE.

The leftover portion of the article is formatted as shown. We present one specific model in Section "The 2-CMEM" together with plots of their PDFs and hrfs. We derive some of its generic reliability features in Section "Reliability Metrics", like MTR, CHRF, Mills Ratio, and MTF. In Section "Estimation inference via simulation", model parameters are estimated using MLE, LSE and WLSE and presents simulation results to evaluate execution of these estimators. To demonstrate the flexibility of the mixture model, we present two applications in Section "Real Data Applications".

The 2-CMEM

A r. v. T has a 2-component finite mixed model if its PDF and CDF can be expressed as:

$$f(t|\breve{\Delta}) = \pi f_1(t|\vartheta_1) + \ddot{\pi} f_2(t|\vartheta_2), \ddot{\pi} = 1-\pi, \tag{1}$$

$$f(t|\breve{\Delta}) = \pi\vartheta_1 \exp\left(-\vartheta_1 t\right) + \ddot{\pi}\vartheta_2 \exp\left(-\vartheta_2 t\right), \tag{2}$$

and

$$F(t|\breve{\Delta}) = \pi F_1(t|\vartheta_1) + \ddot{\pi} F_2(t|\vartheta_2), \tag{3}$$

$$F(t|\breve{\Delta}) = \pi\left\{1-\exp\left(-\vartheta_1 t\right)\right\} + \ddot{\pi}\left\{1-\exp\left(-\vartheta_2 t\right)\right\}, \tag{4}$$

where $\breve{\Delta} = \left(\vartheta_1, \vartheta_2, \pi\right)\vartheta_k, k = 1,2$ are positive scale parameters, while π is mixing parameter.

Fig. 1 gives numerous images of $f(t|\breve{\Delta})$ and $h(t|\breve{\Delta})$ for different characteristics values. The above-mentioned PDF and HRF demonstrate how the parametric vector $(\breve{\Delta})$ affect density of 2-CMEM. It is worth noting that parameter values were picked at random till a broad range of forms for parameters of interest could be captured. As demonstrated in Fig. 1, 2-CMEM can be right skewed. Each exponential distribution's HRF has a constant behaviour, however HRF of 2-CMEM may obviously concede failure rate with declining behaviour, as seen in Fig. 1.

Quantile function

The PDF's features, such as the moments, are likewise determined by the QF. Furthermore, the QF describes the model and can be applied to data evaluation [26]. Suppose that $F(Q_p;\breve{\Delta})$ be CDF of 2-CMEM at pth quantiles. Then the pth quantile of 2-CMEM $r.v.$ is

$$t(p;\breve{\Delta}) = \pi\frac{1}{\vartheta_1}\log(1-p)^{-1} + \ddot{\pi}\frac{1}{\vartheta_2}\log(1-p)^{-1}. \tag{5}$$

Median

The median of 2-CMEM can be found by solving the following equation for t and getting median t^*.

$$\pi\left\{1-\exp\left(-\vartheta_1 t\right)\right\} + \ddot{\pi}\left\{1-\exp\left(-\vartheta_2 t\right)\right\} = 0.5, \tag{6}$$

$$\pi\exp\left(-\vartheta_1 t\right) + \ddot{\pi}\exp\left(-\vartheta_2 t\right) = 0.5. \tag{7}$$

Computational procedures such as Newton–Raphson techniques can be utilized to determine t^* (median) from Eq. (7). The median of 2-CMEM is plotted in Fig. 2. As ϑ_1 grows the median decreases, as shown in this graph.

rth moments about origin

For the r. v. T, rth moments about the origin are:

$$E(T^r) = \int_0^\infty t^r f(t|\breve{\Delta})dt = \int_0^\infty t^r\left\{\pi\vartheta_1\exp\left(-\vartheta_1 t\right) + \ddot{\pi}\vartheta_2\exp\left(-\vartheta_2 t\right)\right\}dt, \tag{8}$$

$$E(T^r) = \pi\frac{\Gamma(r+1)}{\vartheta_1^r} + \ddot{\pi}\frac{\Gamma(r+1)}{\vartheta_2^r}. \tag{9}$$

τth-order negative moments

When $-\tau$ is substituted for r in Eq. (8), the result is τth order negative moments, which are defined as follows:

$$E(T^{-\tau}) = \pi\frac{\Gamma(1-\tau)}{\vartheta_1^{-\tau}} + \ddot{\pi}\frac{\Gamma(1-\tau)}{\vartheta_2^{-\tau}}. \tag{10}$$

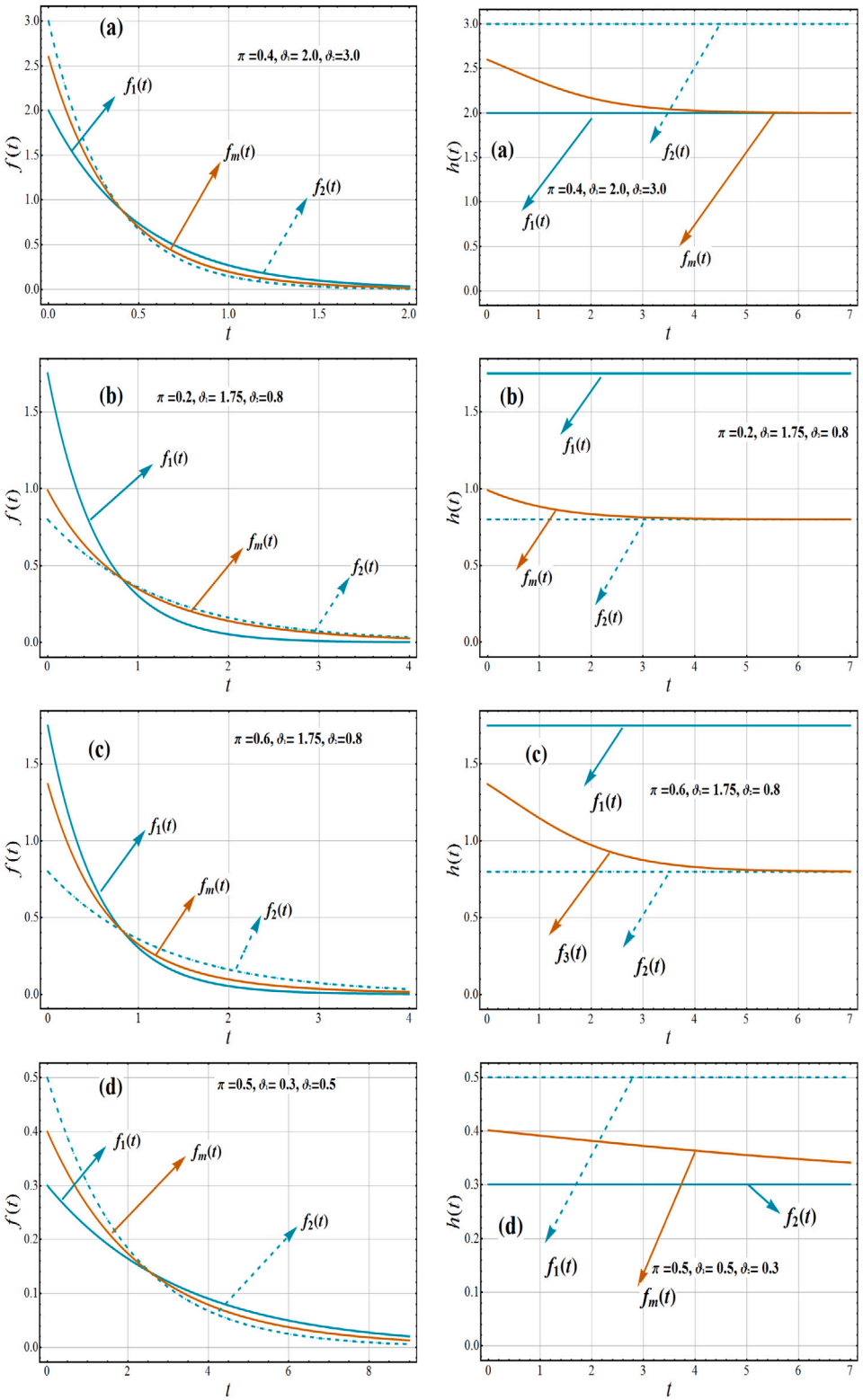

Fig. 1. Variations of first component density ($f_1(t)$), second component density ($f_2(t)$) and variations of $f(t|\breve{\Delta})$ and $h(t|\breve{\Delta})$ of 2-CMEM$(\breve{\Delta})$.

Moment generating function

A 2-CMEM$(\breve{\Delta})$'s MGF is specified as:

$$\tilde{M}_t(\upsilon) = E\left(e^{t\upsilon}\right) = \int_0^{\infty} e^{t\upsilon}\left\{\pi\vartheta_1 \exp\left(-\vartheta_1 t\right) + \ddot{\pi}\vartheta_2 \exp\left(-\vartheta_2 t\right)\right\} dt, \tag{11}$$

$$\tilde{M}_t(\upsilon) = \pi\frac{\vartheta_1}{\left(\vartheta_1 - \upsilon\right)} + \ddot{\pi}\frac{\vartheta_2}{\left(\vartheta_2 - \upsilon\right)}. \tag{12}$$

Characteristic function

By substituting υ with '$i\upsilon$' in Eq. (11), the CF can be determined as

$$\ddot{\tilde{M}}_t(\upsilon) = \pi\frac{\vartheta_1}{\left(\vartheta_1 - i\upsilon\right)} + \ddot{\pi}\frac{\vartheta_2}{\left(\vartheta_2 - i\upsilon\right)}. \tag{13}$$

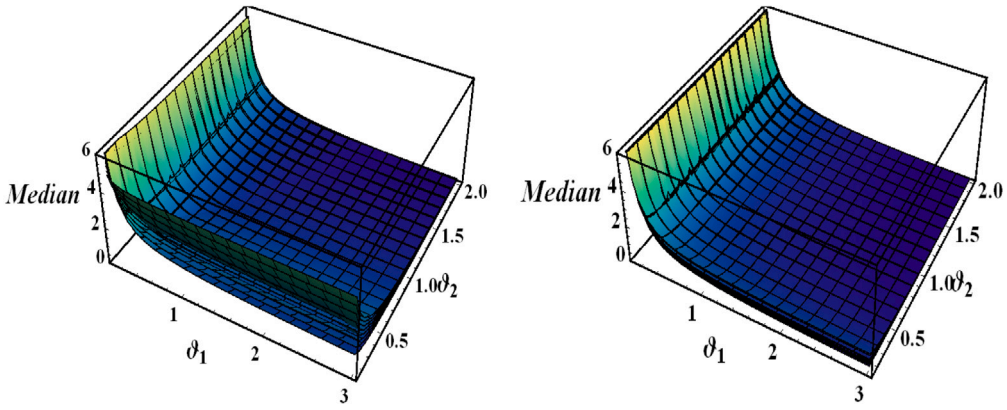

Fig. 2. Variations of median of 2-CMEM($\breve{\Delta}$).

Probability generating function

In Eq. (11), we can get the PGF by substituting υ with "ln(ω)" as follows:

$$P_t(\omega) = E\left(\omega^T\right) = E\left(e^{T\ln\omega}\right) = \pi\frac{\vartheta_1}{\left(\vartheta_1 - \ln\omega\right)} + \ddot{\pi}\frac{\vartheta_2}{\left(\vartheta_2 - \ln\omega\right)}. \tag{14}$$

Factorial moment generating function

By substituting υ with '$\ln(1+\phi)$' in Eq. (11), the FMGF can be determined as

$$F_t(\omega) = E\left((1+\phi)^T\right) = E\left(e^{T\ln(1+\phi)}\right) = \pi\frac{\vartheta_1}{\left[\vartheta_1 - \ln(1+\phi)\right]} + \ddot{\pi}\frac{\vartheta_2}{\left[\vartheta_2 - \ln(1+\phi)\right]}. \tag{15}$$

Reliability metrics

In this part, we will go through some of the most common reliability metrics. In fact, the most important and excellent metrics for a certain gadget must be chosen depending on the manufacturer's originality and function.

Reliability function

Reliability refers to an object's capacity to execute a desired function for a set period of time under specified operating conditions. If TTF is the r.v., and $F(t)$ denotes the FF, then the reliability function $R(t)$ is.

$$R\left(t|\breve{\Delta}\right) = \pi\exp\left(-\vartheta_1 t\right) + \ddot{\pi}\exp\left(-\vartheta_2 t\right). \tag{16}$$

Hazard function

The HRF is a parameter used in reliability theory to compare two different systems. The hazard function is a measure of how the system's reliability is affected by age. It assesses the likelihood of failure as system evolves. The $h(t)$ of 2-CMEM reliability model is

$$h(t|\breve{\Delta}) = \frac{\pi\vartheta_1\exp\left(-\vartheta_1 t\right) + \ddot{\pi}\vartheta_2\exp\left(-\vartheta_2 t\right)}{\pi\exp\left(-\vartheta_1 t\right) + \ddot{\pi}\exp\left(-\vartheta_2 t\right)}. \tag{17}$$

Mills ratio

Mills Ratio of 2-CMEM is.

$$Y\left(t|\breve{\Delta}\right) = \frac{R\left(t|\breve{\Delta}\right)}{f\left(t|\breve{\Delta}\right)} = \frac{\pi\exp\left(-\vartheta_1 t\right) + \ddot{\pi}\exp\left(-\vartheta_2 t\right)}{\pi\vartheta_1\exp\left(-\vartheta_1 t\right) + \ddot{\pi}\vartheta_2\exp\left(-\vartheta_2 t\right)}. \tag{18}$$

The Mills Ratio of 2-CMEM() is presented in Fig. 3. The Mills ratio can be growing or increasing-constant. Individual component density Mills ratio, on the other hand, has a consistent pattern.

Cumulative Hazard rate function

The integrated HRF is another name for the CHRF. The CHRF does not represent a likelihood. However, it is also a risk indicator: the higher $H\left(t|\breve{\Delta}\right)$ value, the greater the risk of collapse by t-time.

$$H(t) = \int_0^t h(y|\breve{\Delta})dy = -\log\left[S(t)\right]. \tag{19}$$

It is important to note that

$$S(t) = e^{-H(t)} \text{and } f(t) = h(t)e^{-H(t)}. \tag{20}$$

Hence,

$$H(t|\breve{\Delta}) = -\log\left[\pi\exp\left(-\vartheta_1 t\right) + \ddot{\pi}\exp\left(-\vartheta_2 t\right)\right]. \tag{21}$$

Fig. 4 portrays the behaviour of $H\left(t|\breve{\Delta}\right)$. The CHRF is a function of ϑ_1, ϑ_2 and π that is rising.

Reversed Hazard rate function

The RHRF has got a lot of interest in the published studies of reliability and stochastic modelling. We refer to [27–29] for definitions, characterizations, and further information.

$$\breve{h}(t|\breve{\Delta}) = \frac{f\left(t|\breve{\Delta}\right)}{F\left(t|\breve{\Delta}\right)} = \frac{\pi\vartheta_1\exp\left(-\vartheta_1 t\right) + \ddot{\pi}\vartheta_2\exp\left(-\vartheta_2 t\right)}{1 - \pi\exp\left(-\vartheta_1 t\right) - \ddot{\pi}\exp\left(-\vartheta_2 t\right)}. \tag{22}$$

At various levels of π, RHRF is a declining function of ϑ_1 and ϑ_2. (see Fig. 5 left). The larger the change in RHRF curve, the lower the inputs of the component ϑ_1 along with ϑ_2. When ϑ_1 approaches 1, RHRF also provides lower values. It is also worth noting that the RHRF curve is a decreasing function of t and ϑ_1 for fixed values of ϑ_2 and (see Fig. 5 right). For fixed values of ϑ_2 and π, the lower the t along ϑ_1 inputs, the higher the change in the RHRF curve.

Mean time to failure

MTTF is reliability term that refer to methodologies and procedures for predicting a product's longevity. When deciding which object to buy for their implementation, users frequently need to consider reliability data. MTTF is methods for calculating a numeric value depending on a set of data in order to quantify a failure rate and time it takes for expected execution to occur. Furthermore, predicting MTTF, is required in addition to make and manufacture a sustainable system. If 2-CMEM($\breve{\Delta}$) then reliability function is used to express MTTF, that is:

$$\ddot{M}\left(t|\breve{\Delta}\right) = \int_0^{+\infty} R(x)\,dx, \tag{23}$$

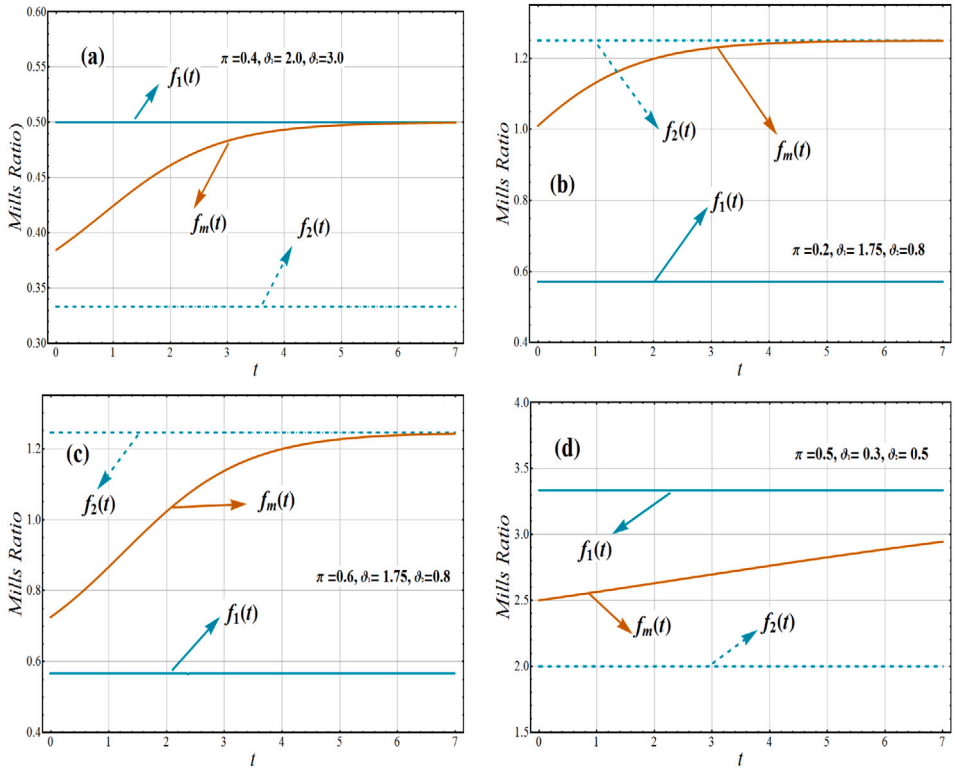

Fig. 3. Variations of Mills Ratio of 2-CMEM$(\breve{\Delta})$ along with ϑ_1, ϑ_2 and π.

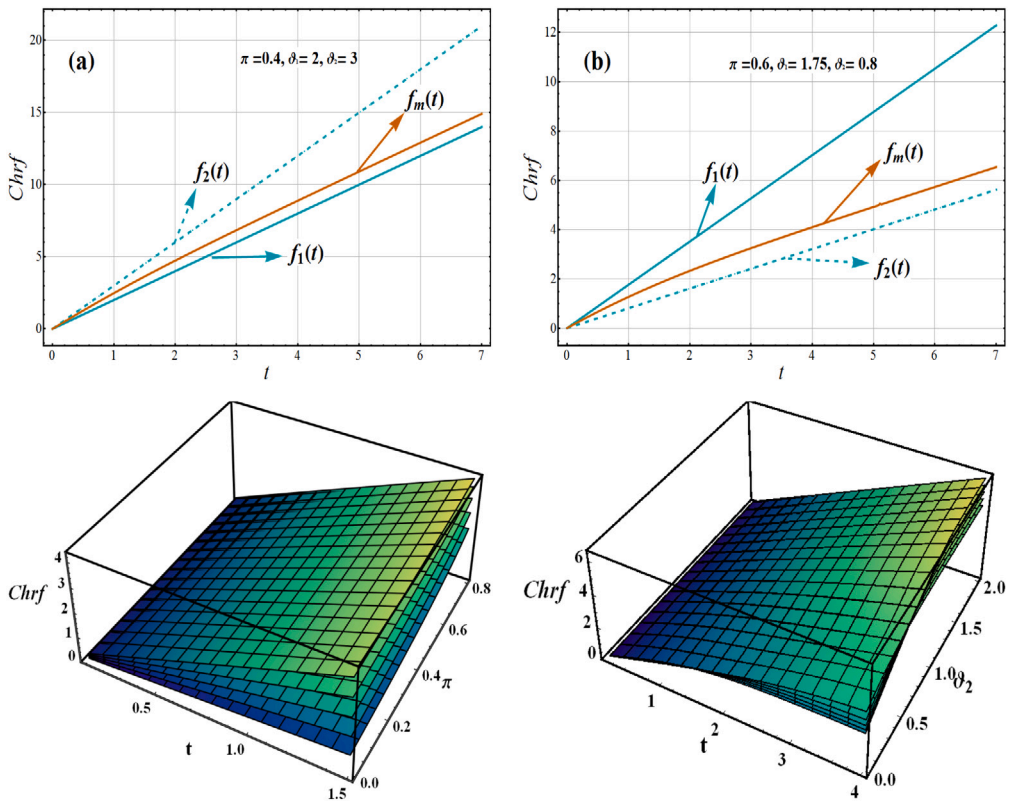

Fig. 4. Fluctuation of $H\,(t|\breve{\Delta})$ of 2-CMEM$(\breve{\Delta})$ along with ϑ_1, ϑ_2 and π.

where $R(t)$ in Eq. (16). Hence

$$\ddot{M}\,(t|\breve{\Delta}) = \frac{\pi}{\vartheta_1} + \frac{\ddot{\pi}}{\vartheta_2}. \tag{24}$$

At different levels of π, MTTF is a decreasing function of ϑ_1 and ϑ_2. (see Fig. 6 left). As the smaller inputs of the parameter ϑ_1 along ϑ_2 contribute the greater variation in MTTF curve. Also MTTF returns

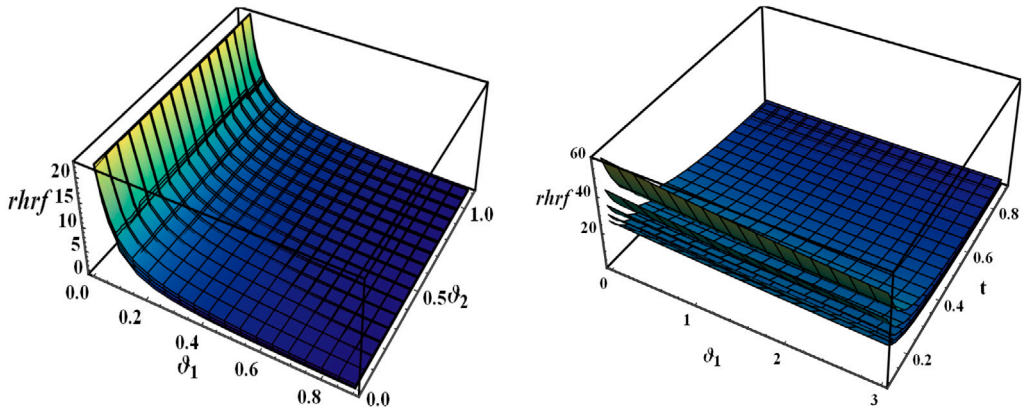

Fig. 5. Fluctuation of $\check{h}(t|\check{\Delta})$ of 2-CMEM$(\check{\Delta})$ along with ϑ_1, ϑ_2 and π.

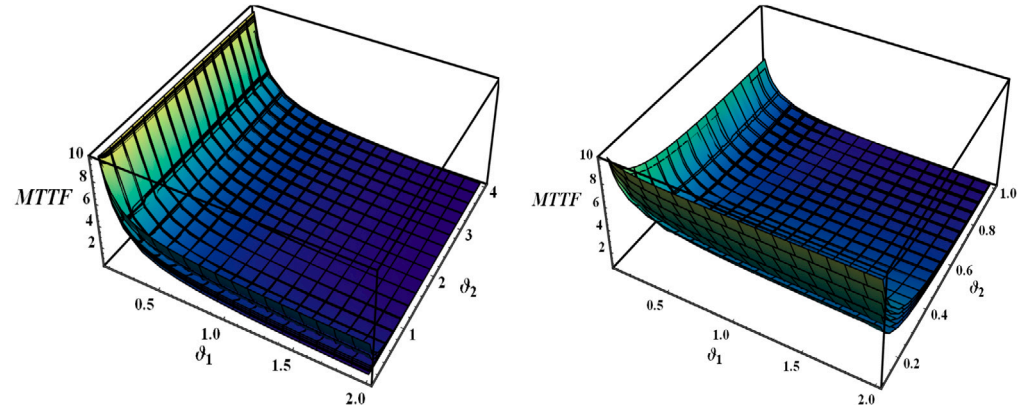

Fig. 6. Fluctuations of $\check{M}_R(t|\check{\Delta})$ of 2-CMEM$(\check{\Delta})$ along with ϑ_1, ϑ_2 and π.

lesser values when ϑ_2 tends to 1. Furthermore, it is mentioned that for fixed values of t and π, the curve of MTTF is a declining function of ϑ_1 and ϑ_2. The greater the shift in MTTF curve, the lesser inputs of the ϑ_2 along t.

Mean Residual Life (MRL)

The remaining lifetime after t for a component of age t is random. The MRL or mean remaining life is expected value of this random residual lifetime and is indicated by $\check{M}_R(t|\check{\Delta})$.

$$\check{M}_R(t|\check{\Delta}) = \frac{1}{R(t)}\int_t^{+\infty} R(x)dx, \tag{25}$$

$$\check{M}_R(t|\check{\Delta}) = \left\{\frac{\pi\exp(-\vartheta_1 t)}{\vartheta_1} + \frac{\ddot{\pi}\exp(-\vartheta_2 t)}{\vartheta_2}\right\} \times \frac{1}{\pi\exp(-\vartheta_1 t) + \ddot{\pi}\exp(-\vartheta_2 t)}. \tag{26}$$

where $R(t)$ in Eq. (16).

$\check{M}_R(t|\check{\Delta})$ is a increasing function of π and t at various levels of ϑ_1 and ϑ_2 (See Fig. 7 on the left). Whereas the curve of MRL is a declining function of ϑ_1 and t.

Estimation inference via simulation

The assessment of parametric vector $\check{\Delta}$ is carried out by the three familiar estimation procedures such as MLE, LSE and WLSE. From now, $t_1, t_2, \ldots, t_n$ symbolize n observed values from T and their ascending ordering values $t_{(1)} \le t_{(2)} \le \ldots \le t_{(n)}$.

Maximum likelihood estimation

The widely known approach of parameter estimate is the maximum likelihood method. The method's popularity is due to its numerous desired qualities, such as consistency, normality and asymptotic efficiency. Let $t_1, t_2, \ldots, t_n$ be n observed values from the Eq. (2) and $\check{\Delta}$ be the vector of unknown parameters. The assessments of MLEs of $\check{\Delta}$ can be provided by optimizing likelihood function with respect to ϑ_1, ϑ_2, and π given by $L(\mathbf{t}|\check{\Delta}) = \prod_{i=1}^n f(t_i;\check{\Delta})$ or likewise the $\log(L(\mathbf{t}|\check{\Delta}))$ for $\check{\Delta}$

$$l(\mathbf{t}|\check{\Delta}) = \ln\prod_{i=1}^n f(t_i;\check{\Delta}), \tag{27}$$

$$l(\mathbf{t}|\check{\Delta}) = \sum_{i=1}^n \ln\left\{\pi\vartheta_1\exp(-\vartheta_1 t_i) + \ddot{\pi}\vartheta_2\exp(-\vartheta_2 t_i)\right\}. \tag{28}$$

So, by partially differentiating $l(\mathbf{t}|\check{\Delta})$ with regard to each of the parameters (ϑ_1, ϑ_2, π) and setting the findings to zero, maximum likelihood estimates of respective parameters are provided, likelihood equations are

$$\frac{\partial l(\mathbf{t}|\check{\Delta})}{\partial\vartheta_1} = \sum_{i=1}^n \frac{\pi\exp(-\vartheta_1 t_i) - \pi\vartheta_1 t_i\exp(-\vartheta_1 t_i)}{\left\{\pi\vartheta_1\exp(-\vartheta_1 t_i) + \ddot{\pi}\vartheta_2\exp(-\vartheta_2 t_i)\right\}}, \tag{29}$$

$$\frac{\partial l(\mathbf{t}|\check{\Delta})}{\partial\vartheta_2} = \sum_{i=1}^n \frac{\ddot{\pi}\exp(-\vartheta_2 t_i) - \ddot{\pi}\vartheta_2 t_i\exp(-\vartheta_2 t_i)}{\left\{\pi\vartheta_1\exp(-\vartheta_1 t_i) + \ddot{\pi}\vartheta_2\exp(-\vartheta_2 t_i)\right\}}, \tag{30}$$

$$\frac{\partial l(\mathbf{t}|\check{\Delta})}{\partial\pi} = \sum_{i=1}^n \frac{\vartheta_1\exp(-\vartheta_1 t_i) - \vartheta_2\exp(-\vartheta_2 t_i)}{\left\{\pi\vartheta_1\exp(-\vartheta_1 t_i) + \ddot{\pi}\vartheta_2\exp(-\vartheta_2 t_i)\right\}}. \tag{31}$$

As a result, solving this nonlinear system of equations gives the MLE. Although these equations cannot be analytically solved, we use statistical software through iterative approach like Newton method or fixed point iteration methods can be used to solve them.

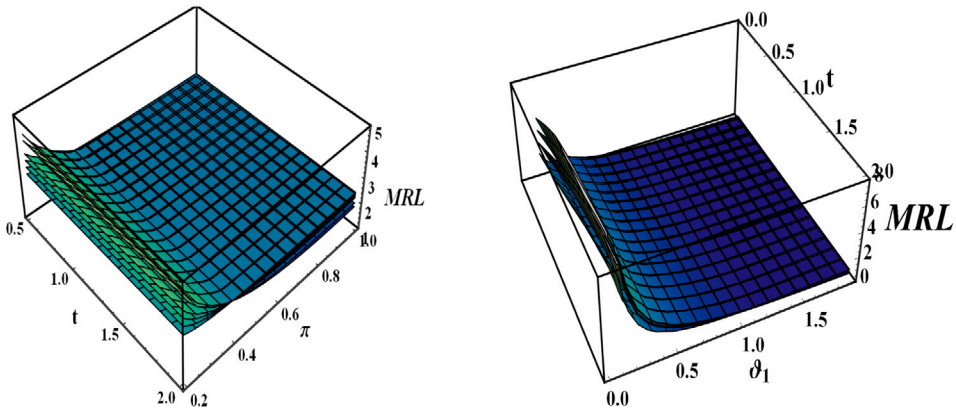

Fig. 7. Fluctuations of $\breve{M}_R(t|\breve{\Delta})$ of 2-CMEM$(\breve{\Delta})$.

Least square estimators

For estimating unknown parameters, the ordinary least square approach is well-known [30]. The least square estimators of ϑ_1, ϑ_2 and π, denoted by $\breve{\vartheta}_{1_{LSE}}, \breve{\vartheta}_{2_{LSE}}$ and $\breve{\pi}_{LSE}$, can be obtained by minimizing the function

$$LS(\breve{\Delta}) = \sum_{i=1}^{n}\left[F(t_{(i)}|\breve{\Delta}) - \frac{i}{n+1}\right]^2, \tag{32}$$

with regard to ϑ_1, ϑ_2 and π, where F$(\cdot)$ is given by Eq. (4). They can be derived in the same way by solving the following equations:

$$\frac{\partial LS(\breve{\Delta})}{\partial \vartheta_1} = \sum_{i=1}^{n}\left[F(t_{(i)}|\breve{\Delta}) - \frac{i}{n+1}\right]\Psi_1(t_{(i)}|\vartheta_1) = 0, \tag{33}$$

$$\frac{\partial LS(\breve{\Delta})}{\partial \vartheta_2} = \sum_{i=1}^{n}\left[F(t_{(i)}|\breve{\Delta}) - \frac{i}{n+1}\right]\Psi_2(t_{(i)}|\vartheta_2) = 0, \tag{34}$$

and

$$\frac{\partial LS(\breve{\Delta})}{\partial \pi} = \sum_{i=1}^{n}\left[F(t_{(i)}|\breve{\Delta}) - \frac{i}{n+1}\right]\Psi_3(t_{(i)}|\pi) = 0, \tag{35}$$

where

$$\Psi_1(t_{(i)}|\vartheta_1) = \pi t_{(i)} \exp\left(-\vartheta_1 t_{(i)}\right), \tag{36}$$

$$\Psi_2(t_{(i)}|\vartheta_2) = \ddot{\pi} t_{(i)} \exp\left(-\vartheta_2 t_{(i)}\right), \tag{37}$$

$$\Psi_3(t_{(i)}|\pi) = \exp\left(-\vartheta_2 t_{(i)}\right) - \exp\left(-\vartheta_1 t_{(i)}\right). \tag{38}$$

Weighted least squares estimators

Consider the weighted function below (see [31])

$$\kappa_i = \frac{(n+1)^2(n+2)}{i(n-i+1)}. \tag{39}$$

The WLSEs $\breve{\vartheta}_{1_{WLSE}}, \breve{\vartheta}_{2_{WLSE}}$ and $\breve{\pi}_{WLSE}$, can be obtained by minimizing the function

$$WLS(\breve{\Delta}) = \sum_{i=1}^{n}\frac{(n+1)^2(n+2)}{i(n-i+1)}\left[F(t_{(i)}|\breve{\Delta}) - \frac{i}{n+1}\right]^2, \tag{40}$$

One can also get these estimators by solving:

$$\frac{\partial WLS(\breve{\Delta})}{\partial \vartheta_1} = \sum_{i=1}^{n}\frac{(n+1)^2(n+2)}{i(n-i+1)}\left[F(t_{(i)}|\breve{\Delta}) - \frac{i}{n+1}\right]\Psi_1(t_{(i)}|\vartheta_1) = 0, \tag{41}$$

$$\frac{\partial WLS(\breve{\Delta})}{\partial \vartheta_2} = \sum_{i=1}^{n}\frac{(n+1)^2(n+2)}{i(n-i+1)}\left[F(t_{(i)}|\breve{\Delta}) - \frac{i}{n+1}\right]\Psi_2(t_{(i)}|\vartheta_2) = 0, \tag{42}$$

and

$$\frac{\partial WLS(\breve{\Delta})}{\partial \pi} = \sum_{i=1}^{n}\frac{(n+1)^2(n+2)}{i(n-i+1)}\left[F(t_{(i)}|\breve{\Delta}) - \frac{i}{n+1}\right]\Psi_3(t_{(i)}|\pi) = 0, \tag{43}$$

where $\Psi_1(t_{(i)}|\vartheta_1)$, $\Psi_2(t_{(i)}|\vartheta_2)$ and $\Psi_3(t_{(i)}|\pi)$ are given in Eqs. (36)–(38).

Simulation study

A brief simulation is run to evaluate the execution of MLE, LSE and WLSE methods for estimating parameters. The estimators of parameters of current model have been evaluated by simulating: $(\vartheta_1, \vartheta_2, \pi) = \{(2, 1.5, 0.4)$ and $(2.3, 2.5, 0.6)\}$. With respect to various sample sizes, we evaluated the MLE, LSE and WLSE approaches' performance. The biases, or MSEs, of parameter estimates are evaluated. The validity of the estimators has been assessed using bias and the MSE of estimators. The efficiency of each parameter estimation approach for the 2-CMEM$(\breve{\Delta})$ model in terms of n is examined. Simulation study is executed for this purpose on the basis of given steps:

1. Using the 2-CMEM$(\breve{\Delta})$, generate 1000 samples of size $n = 10, 20, \ldots, 900$ at various parameter values. We generate we πn and $n(1-\pi)$ observations from exp (ϑ_1) and exp (ϑ_2), respectively.
2. Calculate MLEs, LSEs and WLSEs for 1000 samples, say $\breve{\theta}_j$ for $j = 1, 2, \ldots, 1000$.
3. Calculate biases and MSEs. The accompanying formulas are used to achieve these objectives:

$$Bias_\theta(n) = \frac{1}{1000}\sum_{j=1}^{1000}\left(\breve{\theta}_j - \theta\right),$$

$$MSE_\theta(n) = \frac{1}{1000}\sum_{j=1}^{1000}\left(\breve{\theta}_j - \theta\right)^2,$$

where $\theta = (\vartheta_1, \vartheta_2, \pi)$.

The results of simulations of this subsection is indicated in Figs. 8–11 These empirical findings show that the proposed estimate methods do a fantastic effort of estimating the 2-CMEM parameters. Because the bias approaches to zero as n grows larger, one can conclude that the estimators have asymptotic unbiasedness. The MSE behaviour, on the other hand, indicates consistency because the errors tend to zero as n increases. From Figs. 8–11, the following observations can be extracted.

- The bias of $\breve{\vartheta}_1, \breve{\vartheta}_2, \breve{\pi}$, declines as n grows for all estimation approaches.
- For all estimation approaches, the biases are generally positive except bias of $\breve{\vartheta}_1$ under MLE approach, and bias of $\breve{\pi}$ under WLSE and LSE approaches.
- Under the MLE, the bias of parameters is least than other two approaches (Figs. 8 and 10).
- Under WLSE and LSE approaches, the higher MSE of $\breve{\vartheta}_1, \breve{\vartheta}_2, \breve{\pi}$ are observed (Figs. 9 and 11).
- In terms of bias, generally the performances of the MLE, is the good (Figs. 8–10).
- The estimates under LSE approach are mostly overestimated (Figs. 7 and 11).

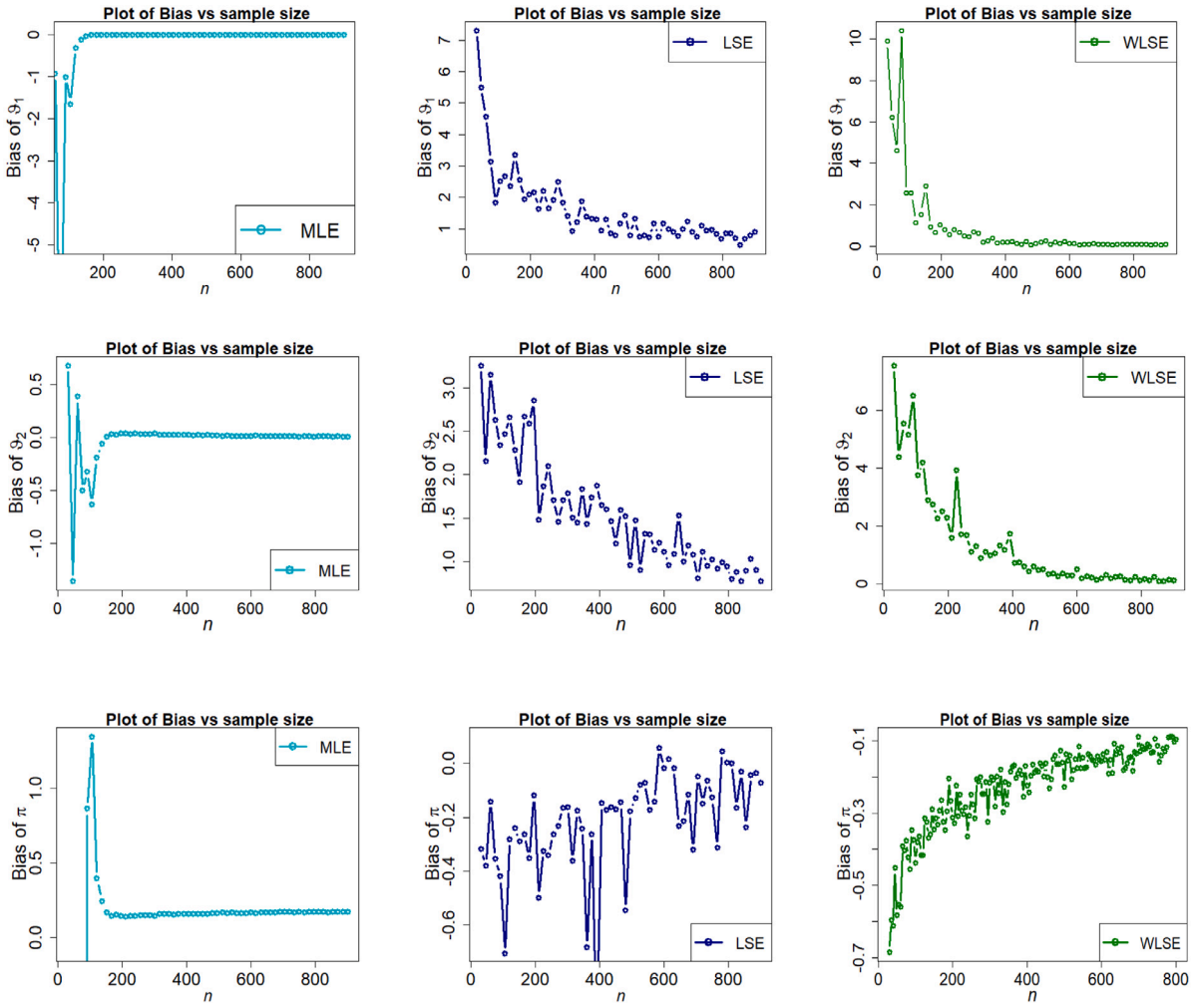

Fig. 8. Fluctuations of bias of estimations under different methods for parametric set I.

- It is noted that difference of estimates from assumed parameters reduce to zero with an increase in n under all estimation approaches.
- When compared to alternative estimation technique, generally the MLE estimation is stronger in terms of bias and MSE for all specified parameter values, when sample size approaches infinity (Figs. 8–11).

The general judgment from previous figures is that as n rises, all bias and MSE graphs for all parameters will approach zero. This confirms the authenticity of these estimating methodologies as well as the numerical computations for the 2-CMEM$(\breve{\Delta})$ distribution parameters.

Real data applications

This section shows how the proposed model can be implemented to real-world data to demonstrate how 2-CMEM works. These data are used to evaluate 2-CMEM's fits to other competing models, including the Exponentiated Exponential Family (EExF) [32], and Exponential (Ex). The goodness-of- fit statistics for this distribution and other contending distributions are studied, and the MLEs of their parameter. To compare the fitted distributions, we use goodness-of-fit metrics like Anderson–Darling (A^*), Cramer–von Mises (W^*), the AIC and BIC criteria, which are used to assess the quality of fitted models, are computed. In general, the lower these statistics are, the better the fit.

Data set I: The application of anxiety data for a sample of 166 ''normal'' women, i.e., women who do not have a disordered, outside of a pathological clinical picture (Towns-ville, Queensland, Australia), is used to demonstrate the use of these distributions in this section, which were firstly reported in [33].

Data set II: The true data set refers to exceeding flood peaks (in m^3 /s) of the Wheaton River near Carcross, Yukon Territory, Canada. The data was examined by Akinsete et al. [34].

Additional data applications can be found in [35–44]. Tables 1–2 provide the MLEs for each data set, together with their standard errors (in parenthesis) and goodness-of-fit (GOF) measures. Tables 1–2 clearly show that the 2-CMEM$(\breve{\Delta})$ is the best of all the models examined. Though the EExF and Ex models have a little edge in specific GOF measures such as BIC, this small advantage is not substantial when the majority of GOF metrics favour the performance of the 2-CMEM$(\breve{\Delta})$. Therefore, we recommend analysing these data sets using the 2-CMEM$(\breve{\Delta})$ model. Using the R function denscomp(), Figs. 12 and 13 show the plots of the pdfs of the fitted models superimposed over the histogram of the real data sets. In comparison to other one component models, the 2-CMEM$(\breve{\Delta})$ provides a very good fit for these data, as seen in the Figures. Using the R function cdfcomp(), the plots of the theoretical cdfs of the fitted distributions are compared to the empirical cdf of the data in Figs. 12–13. The cdf of the 2-CMEM$(\breve{\Delta})$, yet again, is clearly closer to the empirical distribution than any other model. Figs. 12–13 also depict probability–probability (P–P) plots for data sets I and II, respectively, which support the findings of Tables 1–2. Furthermore, the data sets could have come from the 2-CMEM model, according to the study. The log-likelihood function intersects the x-axis at one point in Figs. 14–15, confirming the existence of MLEs. The

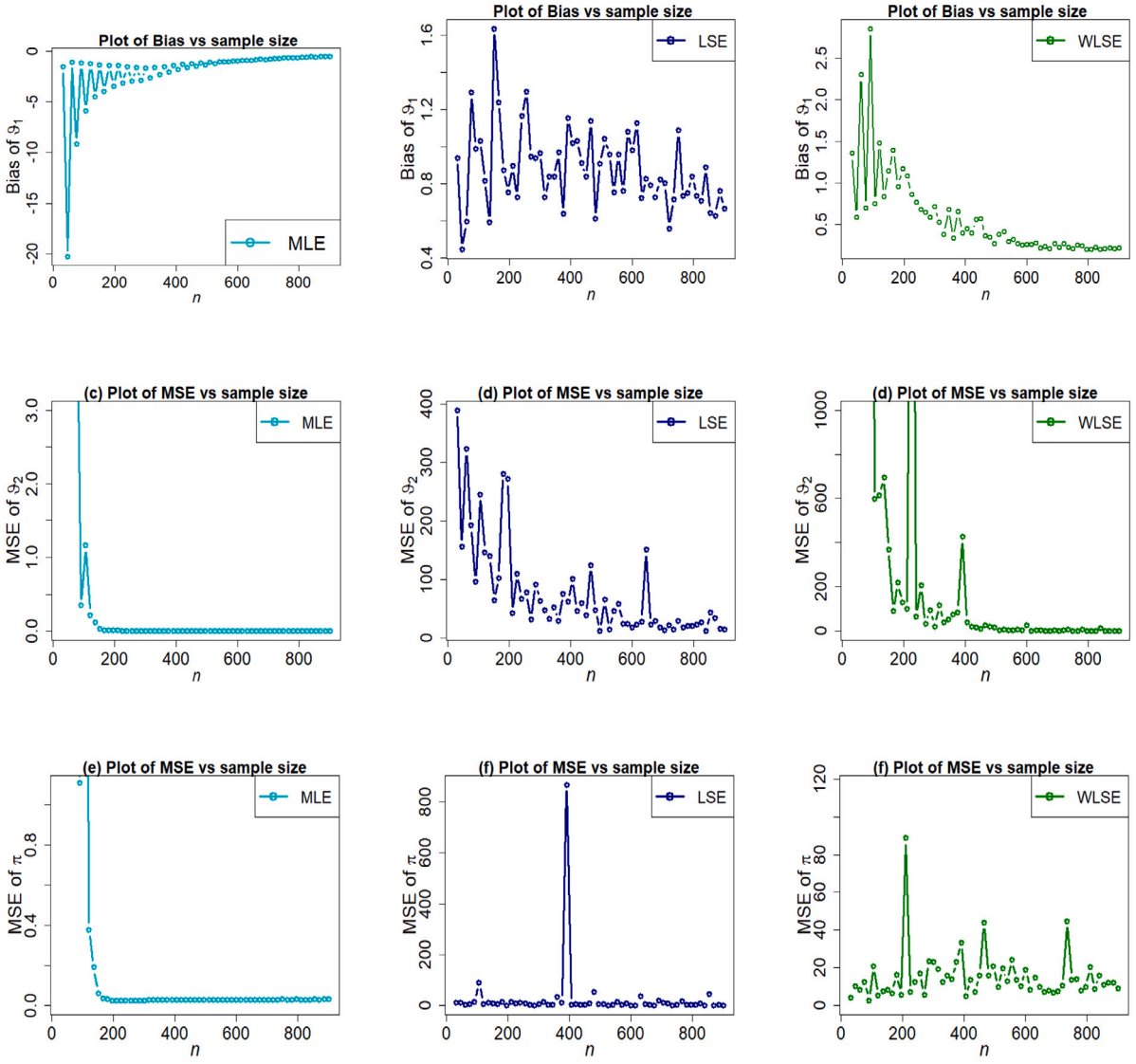

Fig. 9. Fluctuations of MSE of estimators under different methods for parametric set I.

Table 1
MLEs (SEs are given in [ ]), and GOF statistics for the Data set I.

Distributions	MLEs/Standard errors	W^*	A^*	AIC	BIC
2-CMEM $(\vartheta_1, \vartheta_2, \pi)$	6.55295, 78.15756, 0.56084 [0.78959, 15.22897, 0.05665]	2.0591	12.5220	−523.344	−514.009
EExF $(\vartheta_1, \vartheta_2)$	0.64265, 8.02044 [0.06168, 0.93788]	2.0896	12.6267	−482.178	−475.954
Ex(ϑ)	0.09121 [0.00708]	2.0920	12.6438	−461.02	−457.911

fact that the derivative graph is decreasing indicates that the scoring functions of $\vartheta_1, \vartheta_2, \pi$ are changing from increasing to decreasing, and so is at their maximum. Figs. 16–17 show the profiles of the log-likelihood function (PLLF) based on data sets I, and II. Moreover, the MLEs are unique, as the log-likelihood function has a global maximum, as seen in Figs. 16–17.

Conclusion

In survival analysis, the exponential distribution is one of the most popular lifespan distributions. However, in terms of lifespan analysis, the constant behaviour of the hrf of this distribution is a hurdle. In real-world applications, empirical hazard rate curves frequently have non-monotonic shapes. As a result, there is a good reason to look into mixtures or modifications of the exponential distribution that can provide lifespan modelling more flexibility. A mixture of one parameter extreme distributions is presented in this study using three estimate techniques: MLE, LSE, and WLSE. To compare the performance of various estimation methods, a simulation analysis was done by using the R package. A simulation has been executed with various sample sizes, and it was revealed that MLE methodology worked well for estimating parameters for the data sets under consideration. Figs. 14,

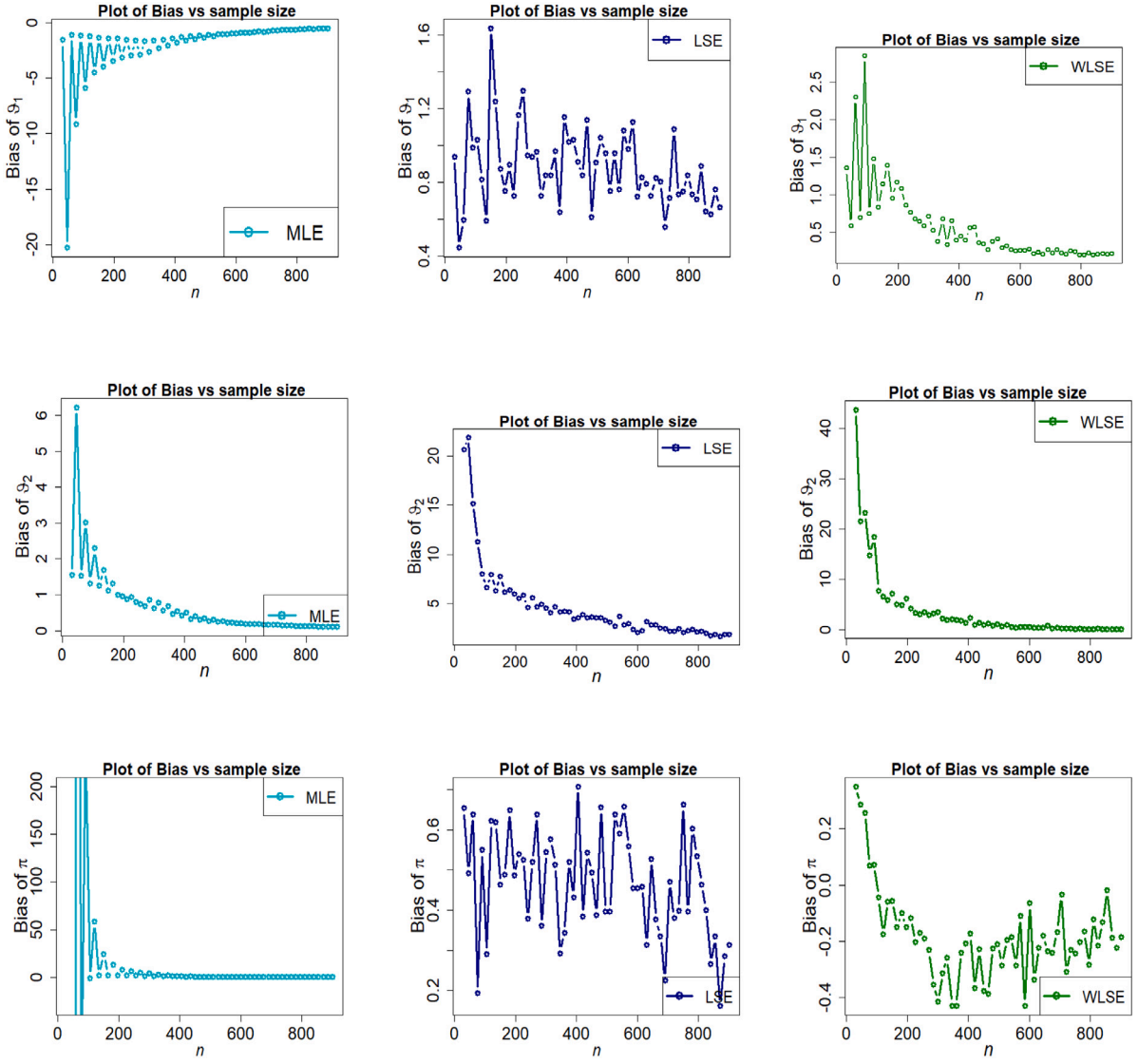

Fig. 10. Fluctuations of bias of estimators under different methods for parametric set II.

Table 2
MLEs (SEs are given in [ ]), and GOF statistics for the Data set II.

Distributions	MLEs/Standard errors	W^*	A^*	AIC	BIC
2-CMEM $(\vartheta_1, \vartheta_2, \pi)$	0.06956, 0.67001, 0.83144 [0.01052, 0.30152, 0.08801]	0.09135	0.52131	505.6434	512.4734
EExF $(\vartheta_1, \vartheta_2)$	0.82839, 0.07243 [0.12309, 0.01170]	0.12862	0.74205	506.5871	511.1404
Ex(ϑ)	12.20416 [1.43827]	0.13055	0.75231	506.2559	508.5326

15 shows the existence of MLEs as the log-likelihood function cross the x-axis at one point. As it is clear that the log-likelihood function is a decreasing function and intersects x-axis at one point. Furthermore, Figs. 16, 17 shows that the log-likelihood function has global maximum roots. Ultimately, two data implementations have been studied to demonstrate the versatility and superiority of the mixture over single component models. For the future work, we can use these estimation techniques for extend mixture model to modelling different real data sets in numbers of area such reliability engineering, survival analysis and so on.

CRediT authorship contribution statement

Showkat Ahmad Lone: Conceptualization, Writing – review & editing, Data curation, Formal analysis, Methodology, Validation, Conceptualization. **Sadia Anwar:** Methodology, Writing – review & editing, Data curation, Formal analysis. **Tabassum Naz Sindhu:** Methodology, Writing – review & editing, Data curation, Formal analysis, Methodology, Validation, Conceptualization. **Fahd Jarad:** Supervision, Writing – review & editing.

Declaration of competing interest

The authors declare that they have no known competing financial interests or personal relationships that could have appeared to influence the work reported in this paper.

Acknowledgements

The authors would like to thank the Editor and anonymous reviewers for their constructive comments that improved the final version of the paper.

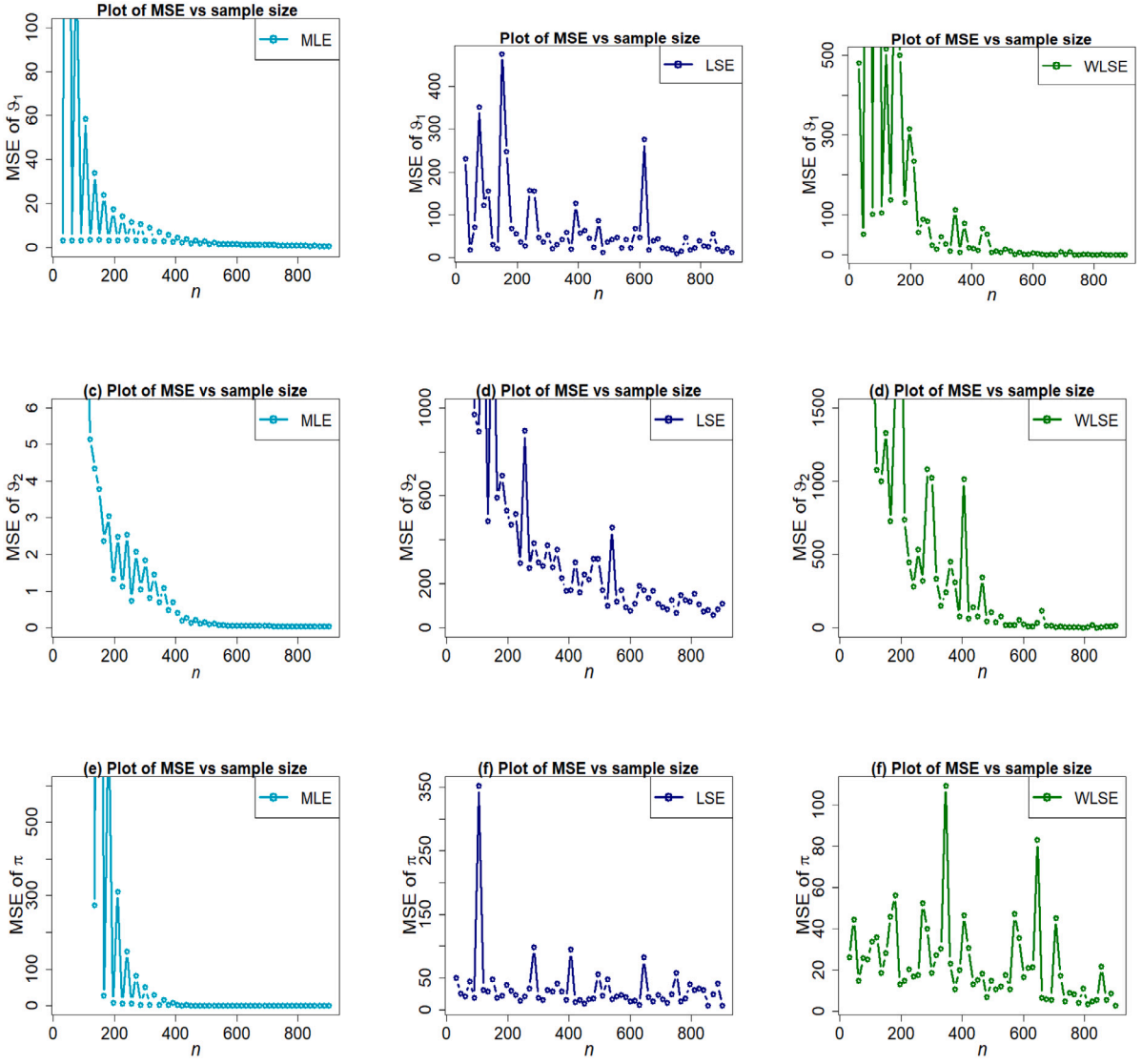

Fig. 11. Fluctuations of MSE of estimators under different methods for parametric set II.

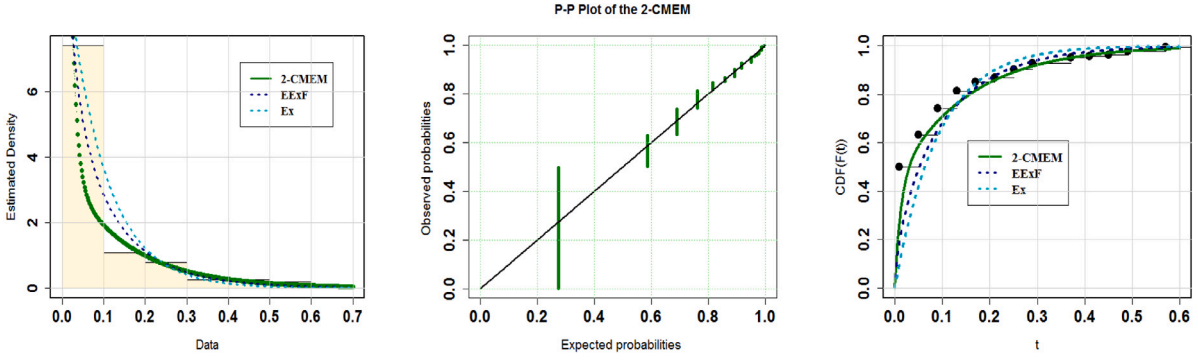

Fig. 12. The ECDF "left panel", PP "middle panel", FPDF "right panel" plots for data set I.

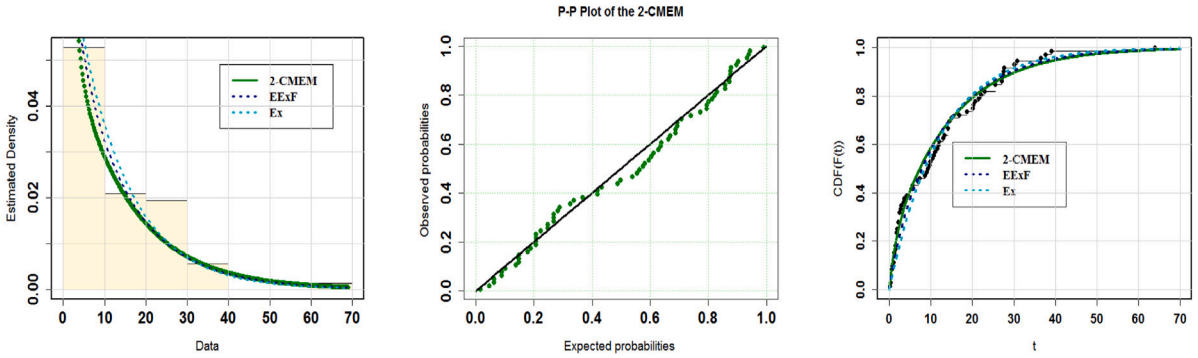

Fig. 13. The ECDF "left panel", PP "middle panel", FPDF "right panel" plots for data set II.

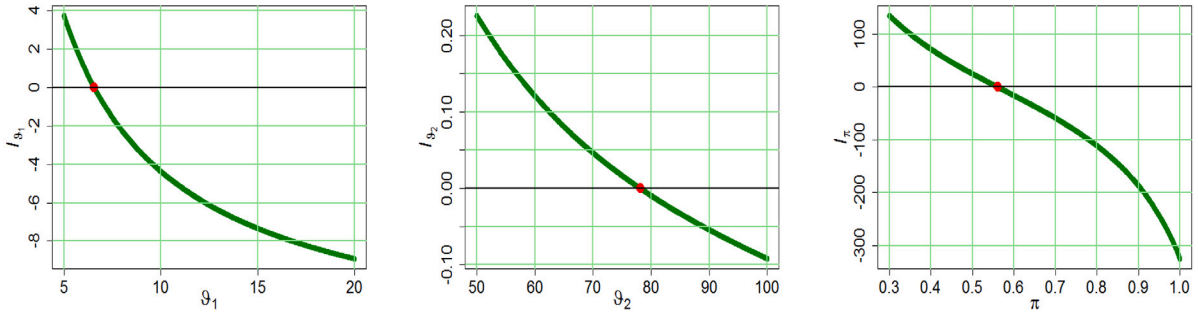

Fig. 14. The graphs of Score functions cross the horizontal axis at $\hat{\vartheta}_1, \hat{\vartheta}_2$, and $\hat{\pi}$ of data set I.

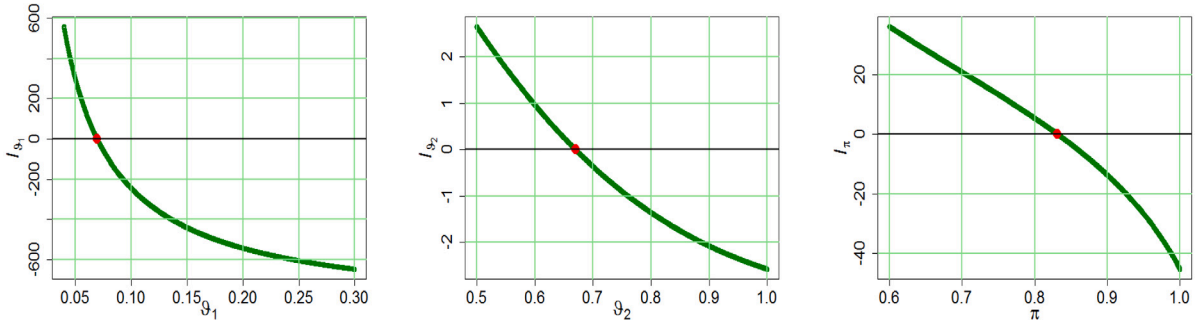

Fig. 15. The graphs of Score functions cross the horizontal axis at $\hat{\vartheta}_1, \hat{\vartheta}_2$, and $\hat{\pi}$ of data set II.

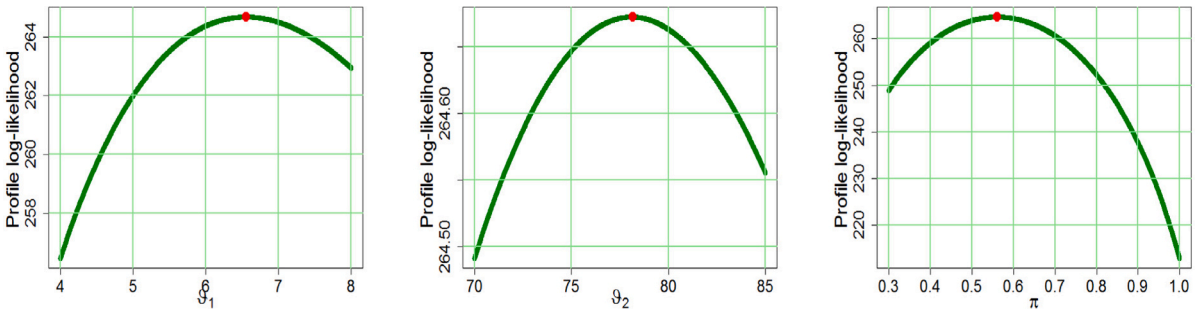

Fig. 16. Curves of profile-likelihood function of three estimated parameters of 2-CMEM model for first real data set.

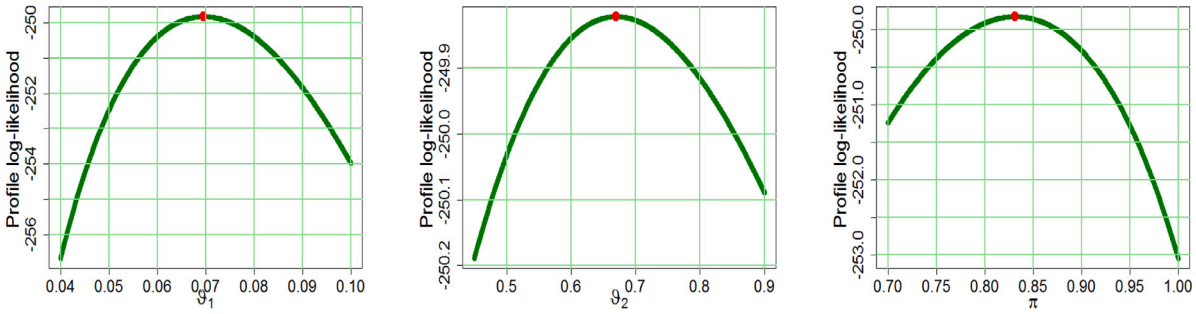

Fig. 17. Curves of profile-likelihood function of three estimated parameters of 2-CMEM model for second real data set.

References

[1] Mohammad D, Muhammad A. On the mixture of BurrXII and Weibull distribution. J Statist Appl Probab J Statist Appl Probab 2014;3:251–67.

[2] Yakowitz SJ, Spragins JD. On the identifiability of finite mixtures. Ann Math Stat 1968;39(1):209–14.

[3] Sultan KS, Ismail MA, Al-Moisheer AS. Mixture of two inverse Weibull distributions: Properties and estimation. Comput Statist Data Anal 2007;51(11):5377–87.

[4] Jiang R, Murthy DNP, Ji P. Models involving two inverse Weibull distributions. Reliab Eng Syst Saf 2001;73(1):73–81.

[5] Mohammadi A, Salehi-Rad MR, Wit EC. Using mixture of Gamma distributions for Bayesian analysis in an M/G/1 queue with optional second service. Comput Statist 2013;28(2):683–700.

[6] Ateya SF. Maximum likelihood estimation under a finite mixture of generalized exponential distributions based on censored data. Statist Papers 2014;55(2):311–25.

[7] Mohamed MM, Saleh E, Helmy SM. Bayesian prediction under a finite mixture of generalized exponential lifetime model. Pak J Statist Oper Res 2014;417–33.

[8] Sindhu TN, Aslam M. Preference of prior for Bayesian analysis of the mixed burr type X distribution under type I censored samples. Pak J Statist Oper Res 2014;17–39.

[9] Zhang H, Huang Y. Finite mixture models and their applications: A review. Austin Biomet Biostat 2015;2(1):1–6.

[10] Sindhu TN, Riaz M, Aslam M, Ahmed Z. Bayes estimation of gumbel mixture models with industrial applications. Trans Inst Meas Control 2016;38(2):201–14.

[11] Sindhu TN, Aslam M, Hussain Z. A simulation study of parameters for the censored shifted Gompertz mixture distribution: A Bayesian approach. J Statist Manage Syst 2016;19(3):423–50.

[12] Sindhu TN, Feroze N, Aslam M, Shafiq A. Bayesian inference of mixture of two Rayleigh distributions: a new look. Punjab Univ J Math 2020;48(2).

[13] Sindhu TN, Khan HM, Hussain Z, Al-Zahrani B. BayesIan inference from the mixture of half-normal distributions under censoring. J Natl Sci Found Sri Lanka 2018;46(4):587–600.

[14] Sindhu TN, Hussain Z, Aslam M. Parameter and reliability estimation of inverted Maxwell mixture model. J Statist Manage Syst 2019;22(3):459–93.

[15] Ali S. Mixture of the inverse Rayleigh distribution: Properties and estimation in a Bayesian framework. Appl Math Model 2015;39(2):515–30.

[16] Tahir M, Aslam M, Abid M, Ali S, Ahsanullah M. A 3-component mixture of exponential distribution assuming doubly censored data: properties and Bayesian estimation. J Stat Theory Appl 2020;19(2):197–211.

[17] Majeed MY, Aslam M. Bayesian analysis of the two component mixture of inverted exponential distribution under quadratic loss function. Int J Phys Sci 2012;7(9):1424–34.

[18] Nair MT, Abdul SE. Finite mixture of exponential model and its applications to renewal and reliability theory. J Stat Theory Pract 2010;4(3):367–73.

[19] Nassar MM. Two properties of mixtures of exponential distributions. IEEE Trans Reliab 1988;37(4):383–5.

[20] Nassar MM, Mahmoud MR. On characterizations of a mixture of exponential distributions. IEEE Trans Reliab 1985;34(5):484–8.

[21] Dey S, Kumar D, Ramos PL, Louzada F. Exponentiated chen distribution: properties and estimation. Comm Statist Simulation Comput 2017;46:8118–39.

[22] Dey S, Alzaatreh A, Zhang C, Kumar D. A new extension of generalized exponential distribution with application to ozone data. Ozone Sci Eng 2017;39(4):273–85.

[23] Dey S, Josmar MJ, Nadarajah S. Kumaraswamy distribution: different methods of estimation. Comput Appl Math 2017. http://dx.doi.org/10.1007/s40314-017-0441-1.

[24] Dey S, Moala FA, Kumar D. Statistical properties and different methods of estimation of gompertz distribution with application. J Statist Manage Syst 2018;21(5):839–76.

[25] Rodrigues GC, Louzada F, Ramos PL. Poisson exponential distribution: different methods of estimation. J Appl Stat 2018;45:128–44.

[26] Nair NU, Sankaran PG, Balakrishnan N. Quantile-based reliability analysis. Statist Ind Technol 2013;29–58. http://dx.doi.org/10.1007/978-0-8176-8361-0.

[27] An MY. Logconcavity versus logconvexity: a complete characterization. J Econom Theory 1998;80(2):350–69.

[28] Bagnoli M, Bergstrom T. Log-concave probability and its applications. Econom Theory 2005;26(2):445–69.

[29] András S, Baricz Á. Properties of the probability density function of the non-central chi-squared distribution. J Math Anal Appl 2008;346(2):395–402.

[30] Swain JJ, Venkatraman S, Wilson JR. Least-squares estimation of distribution functions in Johnson's translation system. J Stat Comput Simul 1988;29(4):271–97.

[31] Gupta RD, Kundu D. Generalized exponential distribution: different method of estimations. J Stat Comput Simul 2001;69(4):315–37.

[32] Gupta RD, Kundu D. Exponentiated exponential family: an alternative to gamma and Weibull distributions. Biomet J: J Math Methods Biosci 2001;43(1):117–30.

[33] Smithson M, Verkuilen J. A better lemon squeezer? Maximum-likelihood regression with beta-distributed dependent variables. Psychol Methods 2006;11(1):54.

[34] Akinsete A, Famoye F, Lee C. The beta-Pareto distribution. Statistics 2008;42(6):547–63.

[35] Sindhu TN, Shafiq A, Al-Mdallal QM. On the analysis of number of deaths due to covid- 19 outbreak data using a new class of distributions. Results Phys 2021;21:103747.

[36] Lone SA, Sindhu TN, Shafiq A, Jarad F. A novel extended gumbel type II model with statistical inference and Covid-19 applications. Results Phys 2022;105377.

[37] Sindhu TN, Hussain Z, Alotaibi N, Muhammad T. Estimation method of mixture distribution and modeling of COVID-19 pandemic. AIMS Math 2022;7(6):9926–56.

[38] Lone SA, Sindhu TN, Jarad F. Additive trinomial Fréchet distribution with practical application. Results Phys 2022;33:105087.

[39] Shafiq A, Lone SA, Sindhu TN, El Khatib Y, Al-Mdallal QM, Muhammad T. A new modified kies Fréchet distribution: Applications of mortality rate of Covid-19. Results Phys 2021;28:104638.

[40] Shafiq Anum, Sindhu Tabassum Naz, Alotaibi Naif. A novel extended model with versatile shaped failure rate: Statistical inference with Covid-19 applications. Results Phys 2022;105398.

[41] Sindhu TN, Shafiq A, Al-Mdallal QM. Exponentiated transformation of gumbel type-II distribution for modeling COVID-19 data. Alexandria Eng J 2021;60(1):671–89.

[42] Baba IA, Ahmed I, Al-Mdallal QM, Jarad F, Yunusa S. Numerical and theoretical analysis of an awareness COVID-19 epidemic model via generalized Atangana-Baleanu fractional derivative. J Appl Math Comput Mech 2022;21(1):7–18.

[43] Umar M, Kusen, Raja MAZ, Sabir Z, Al-Mdallal Q. A computational framework to solve the nonlinear dengue fever SIR system. Comput Methods Biomech Biomed Eng 2022;1–14.

[44] Asif M, Jan SU, Haider N, Al-Mdallal Q, Abdeljawad T. Numerical modeling of npz and sir models with and without diffusion. Results Phys 2020;19:103512.